Experimental Parasitology 171 (2016) 23–32

Contents lists available at ScienceDirect

Experimental Parasitology

journal homepage: www.elsevier.com/locate/yexpr

Full length article

Pentamidine antagonizes the benznidazole's effect *in vitro*, and lacks of synergy *in vivo*: Implications about the polyamine transport as an anti-*Trypanosoma cruzi* target

Verónica Seguel [a, 3], Lorena Castro [a, 3], Chantal Reigada [b], Leonel Cortes [a], María V. Díaz [a], Mariana R. Miranda [b], Claudio A. Pereira [b], Michel Lapier [a], Carolina Campos-Estrada [a, 1], Antonio Morello [a], Ulrike Kemmerling [c], Juan D. Maya [a, 4], Rodrigo López-Muñoz [a, *, 2, 4]

[a] Programa de Farmacología Molecular y Clínica, ICBM, Facultad de Medicina, Universidad de Chile, Santiago, Chile
[b] Laboratorio de Parasitología Molecular, Instituto de Investigaciones Médicas Alfredo Lanari, Universidad de Buenos Aires and CONICET, Buenos Aires, Argentina
[c] Programa de Anatomía y Biología del Desarrollo, ICBM, Facultad de Medicina, Universidad de Chile, Santiago, Chile

HIGHLIGHTS

- Pentamidine antagonize the anti-*T. cruzi* effect benznidazole in isolated trypomastigotes and infected cells.
- Pentamidine lack of synergy with benznidazole in *T. cruzi*-infected mice.
- Pentamidine blocks the TcPAT12, but is unable to decrease the trypanothione levels.
- Overexpression of TcPAT12 doesn't modify the effect of pentamidine.

GRAPHICAL ABSTRACT

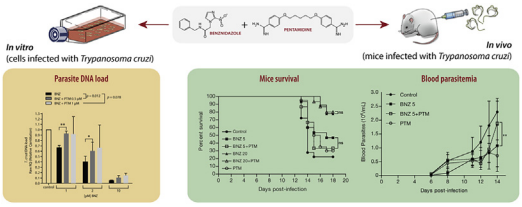

ARTICLE INFO

Article history:
Received 22 March 2016
Received in revised form
2 September 2016
Accepted 6 October 2016
Available online 8 October 2016

Keywords:
Trypanosoma cruzi
Chagas disease
Pentamidine
Benznidazole
Polyamine transport

ABSTRACT

Benznidazole is the first-line drug used in treating Chagas disease, which is caused by the parasite *Trypanosoma cruzi (T. cruzi)*. However, benznidazole has limited efficacy and several adverse reactions. Pentamidine is an antiprotozoal drug used in the treatment of leishmaniasis and African trypanosomiasis. In *T. cruzi*, pentamidine blocks the transport of putrescine, a precursor of trypanothione, which constitutes an essential molecule in the resistance of *T. cruzi* to benznidazole. In the present study, we describe the effect of the combination of benznidazole and pentamidine on isolated parasites, mammalian cells and in mice infected with *T. cruzi*. In isolated trypomastigotes, we performed a dose-matrix scheme of combinations, where pentamidine antagonized the effect of benznidazole, mainly at concentrations below the EC_{50} of pentamidine. In *T. cruzi*-infected mammalian cells, pentamidine reversed the effect of benznidazole (measured by qPCR). In comparison, in infected BALB/c mice, pentamidine failed to get synergy with benznidazole, measured on mice survival, parasitemia and amastigote nest quantification. To further explain the *in vitro* antagonism, we explored whether pentamidine affects intracellular trypanothione levels, however, pentamidine produced no change in trypanothione concentrations. Finally, the *T. cruzi* polyamine permease (TcPAT12) was overexpressed in epimastigotes,

* Corresponding author.
E-mail address: rodrigo.lopez@uach.cl (R. López-Muñoz).
[1] Present address: Facultad de Farmacia, Universidad de Valparaíso, Valparaíso, Chile.
[2] Present address: Instituto de Farmacología y Morfofisiología, Facultad de Ciencias Veterinarias, Universidad Austral de Chile, Valdivia, Chile.
[3] Both authors contributed equally to this work.
[4] Both authors contributed equally to this work.

http://dx.doi.org/10.1016/j.exppara.2016.10.007

showing that pentamidine has the same trypanocidal effect, independently of transporter expression levels. These results suggest that, in spite of the high potency in the putrescine transport blockade, TcPAT12 permease is not the main target of pentamidine, and could explain the lack of synergism between pentamidine and benznidazole.

1. Introduction

American trypanosomiasis (Chagas disease, CD) is a parasitic illness caused by the flagellate protozoan *Trypanosoma cruzi* (*T. cruzi*) (Chagas, 1909). In Latin America, Chagas disease is a leading health problem, being a vector-borne disease with the second highest prevalence and mortality after malaria. In addition, the chronicity of this pathology implies great health expenditures due to the disability associated with this chronic state, which induces heart failure as the main disabling condition (WHO/NTD et al., 2010).

At present, the only drugs used for the treatment of Chagas disease are nifurtimox and benznidazole. Benznidazole (BNZ) is used as the first-line treatment for the disease in all South-American countries. Regardless of its long-lasting use over 50 years, just in 2015 the first randomized clinical trial, evaluating the safety and efficacy of benznidazole, was published, with no favorable results regarding the effectiveness of benznidazole over primary outcomes of the Chagas disease, such as cardiac manifestations (Morillo et al., 2015). In addition, currently is being performed a second trial in Argentina (Riarte, 2013), but their results have yet to be published. Thus, it is imperative to explore other strategies to eliminate the parasite, for instance through the improvement of the benznidazole's effect.

Benznidazole's mechanism of action is not completely understood. There is strong evidence indicating the activation of the prodrug by the type I nitroreductase of *T. cruzi* (TcNTR) (Hall and Wilkinson, 2012). Indeed, spontaneous mutations of the *TcNTR* gene induce benznidazole resistance (Mejia et al., 2012). However, there are other resistance mechanisms described. For instance, there is evidence indicating that trypanothione ($T(SH)_2$), a unique thiol in trypanosomatides, also plays an essential role in benznidazole resistance (Trochine et al., 2014). $T(SH)_2$ is synthesized by the covalent linkage of two molecules of glutathione (GSH) and one of spermidine (a polyamine) (Fairlamb et al., 1985). In this setting, molecules that alter glutathione synthesis, such as buthionine sulfoximine, an inhibitor of GSH synthesis, increase the activity of BNZ (Faundez et al., 2005, 2008). Because $T(SH)_2$ synthesis is also linked to polyamine metabolism, drugs that interfere with polyamine synthesis or uptake can also increase benznidazole's effect.

Polyamines (putrescine, spermidine and spermine) are essential molecules for eukaryotic cells. They are involved in several processes associated with cell replication and DNA stability. In addition, in trypanosomatids (such as *T. cruzi*), spermidine is used for synthesizing $T(SH)_2$, a pivotal molecule in the parasite's antioxidant defense (Manta et al., 2013). In turn, spermidine is produced from putrescine, which is successively synthetized from ornithine in all eukaryotic cells, with the only exception of *T. cruzi*. Thus, given that *T. cruzi* is unable to synthesize putrescine *de novo*, their putrescine availability depends exclusively on transport processes, which could be blocked by drugs such as pentamidine (Diaz et al., 2014).

Pentamidine (4,4'-[pentane-1,5-diylbis(oxy)] dibenzenecarboximidamide), an aromatic diamidine, is a broad-spectrum antiparasitic drug used for decades against leishmaniasis, African trypanosomiasis and some fungi such as *Pneumocystis jirovecii* (Wilkinson and Kelly, 2009). Pentamidine blocks putrescine and spermidine transport in *T. cruzi*. In addition, pentamidine exerts trypanocidal activity *in vitro*, with similar potency as nifurtimox, and decreases parasite load and inflammation in the hearts of infected mice (Diaz et al., 2014).

In the present study, we evaluated the activity of the combination of pentamidine and benznidazole *in vitro*, and in an *in vivo* infection model. In addition, we explored the trypanothione levels in the parasites and the association between the effect of pentamidine and the transport of putrescine in parasites that overexpress the putrescine permease TcPAT12.

2. Materials and methods

2.1. Ethics statement

All animal handling protocols were performed according to the "Guide for the Care and Use of Laboratory Animals" from the National Institutes of Health, USA (National Research Council (U.S.). Committee for the Update of the Guide for the Care and Use of Laboratory Animals. et al., 2011), and were approved by the Institutional Ethical Committee at the Faculty of Medicine, University of Chile (Protocol CBA# 0448 FMUCH) approved for research involved in the FONDECYT-Chile grant #11110182.

2.2. Parasites

Stock cultures of *T. cruzi* epimastigotes (Y strain, DTUs: *T. cruzi* II) were maintained in axenic conditions at 28 °C in BHT (brain-heart-tryptose) media (pH 7) supplemented with 10% fetal calf serum, 100 U/mL penicillin, and 100 mg/L streptomycin (Camargo, 1964). Trypomastigotes were obtained from infected VERO cells (*Chlorocebus sabaeus* kidney fibroblasts, purchased from the ATCC, ATCC number: CCL-81). VERO cells were exposed to trypomastigotes at a 3:1 ratio (trypomastigote:VERO cell). Trypomastigotes were allowed to infect cells for 24 h, after which the supernatant was removed. After a four-day replication cycle, trypomastigotes were released from VERO cells. The parasites were harvested, counted in a Neubauer chamber and used for viability assays.

2.3. TcPAT12 overexpression model

TcPAT12 (gene bank access: AAS47060.1) and *GFP* genes were subcloned into the pTREX expression plasmid (Vazquez and Levin, 1999). Constructions were transfected into *T. cruzi* epimastigotes of Y strain as follows: 10^8 parasites grown at 28 °C in LIT medium were harvested by centrifugation, washed with PBS, and resuspended in 0.35 mL of electroporation buffer (PBS containing 0.5 mM $MgCl_2$ and 0.1 mM $CaCl_2$). This cell suspension was mixed with 50 μg of plasmid DNA in 0.2 cm gap cuvettes (Bio-Rad Laboratories). The parasites were electroporated using a single pulse of 400 V, 500 μF, with a time constant of about 5 ms.

2.4. Parasite viability measurements

The effect of the drug on trypomastigote viability was evaluated through the tetrazolium salt (MTT) reduction assay (Mosmann, 1983). Briefly, 10 μL of 5 mg/mL MTT dye (3[4,5-dimethylthiazol-2-yl]-2,5-diphenyltetrazolium bromide) plus 0.22 mg/mL phenazine methosulfate (used as an electron carrier) were added to each well containing 10^6 parasites in 100 μL of RPMI 1640 medium, without phenol red. After incubating the cells for 4 h at 37 °C, the generated formazan crystals were dissolved with 100 μL of 10% (w/v) SDS in 0.01 M HCl. The plates were kept overnight at 37 °C, and the optical density (OD) was determined using a microplate reader (Labsystems Multiskan MS, Finland) at 570 nm. Under these conditions, the OD is directly proportional to the viable cell number in each well (Díaz-Urrutia et al., 2012; Faundez et al., 2005). For epimastigote parasites, viability was assessed by direct microscopic examination. We exposed 3×10^3 parasites/mL at different conditions and counted them after 5 days in a hemocytometer. All experiments were performed at least three times.

2.5. In vitro infection model

RAW 264.7 cells (murine macrophages, ATCC number CRL-2922) were cultured at a density of 250,000 cells/cm^2, in RPMI 1640 medium supplemented with 5% fetal bovine serum, in a humidified atmosphere with 5% CO_2 at 37 °C. RAW cells were infected with *T. cruzi* trypomastigotes (Y strain) at a 3:1 ratio (trypomastigote:RAW cell). Trypomastigotes were allowed to infect cells for 24 h, after which the supernatant was removed and the medium was replaced with fresh medium with the respective treatments. After 48 h of treatment, cells were harvested by scraping, and DNA was isolated using the Wizard Genomic DNA Purification Kit (Promega, USA), following the manufacturer's instructions.

2.6. In vivo infection model

Adult male BALB/c mice (20–25 g) were obtained from the Central Animal Facility and were maintained in the Animal House of the Pharmacology Program, at the Faculty of Medicine, University of Chile. Animals were maintained in groups of six animals, in polycarbonate clear cages, with food and water *ad libitum*. The animals were infected by intraperitoneal route with 30,000 *T. cruzi* bloodstream trypomastigotes (Y strain). For this purpose, mice received 0.5 mL of blood (with sodium citrate at 2.8%), from previously infected mice. Mice were monitored daily for survival, and signs of distress were recorded following a rated surveillance protocol approved by the Institutional Ethical Committee at the Faculty of Medicine, in accordance with the NIH-USA guidelines (National Research Council (U.S.). Committee for the Update of the Guide for the Care and Use of Laboratory Animals et al., 2011). Animals that obtained the highest scores (15–20 points) were euthanized. For this purpose, mice were anesthetized with an intraperitoneal injection of a ketamine/xylazine mixture (85/30 mg/kg) and euthanized by cervical dislocation. Ketamine was obtained from Drug Pharma Invetec, Chile, whereas xylazine was obtained from Alfasan Laboratories, Argentina. Animals reaching a score equivalent to 10–14 points were placed on acetaminophen treatment to ameliorate suffering. Acetaminophen was chosen because other NSAIDs could interfere with the outcome of Chagas disease in this model of infection (Molina-Berríos et al., 2013a,b,c). To complete the qPCR and histology analyses, surviving mice at day 18 post-infection had to be euthanized.

2.7. Mouse treatments

Mice were treated with 5 or 20 mg/kg/day benznidazole for 15 days, starting on the second day post infection (dpi). The drug was suspended in aqueous 1% methylcellulose and administered by oral gavage (Molina-Berrios, et al., 2013a,b,c). The control mice only received the vehicle. Pentamidine was administered by intraperitoneal route, at 4 mg/kg/day. The drug was dissolved in normal saline solution and was administered in a volume of 100 μL (Diaz et al., 2014). The experiments were performed twice, with 6 experimental groups each (including a control group) and 6 randomized mice for each group.

2.8. Parasite load quantification by qPCR

DNA from infected RAW cells or cardiac tissue from infected mice was isolated using the Wizard Genomic DNA Purification Kit (Promega, USA), following the manufacturer's instructions. DNA was quantified by absorbance measurement at 280 nm, using a Varioskan spectrophotometer (Thermo Scientific, USA). To evaluate the parasite DNA load, we used a TaqMan-Duplex system as we previously described (Molina-Berrios, et al., 2013a,b,c). To amplify an 84-bp *T. cruzi* satellite DNA sequence, the following primers were used: TcSt 4-Fw (5′-GGACCACAACGTGTGATGCA-3′) and TcSt 1-Rev (5′-AGGAATTTCGCGAGCTCTTG-3′) and the TcSt-1 probe (5′-FAM-ATCAGCCGAGTGCAGCACCCTTG-BHQ-1-3′). As an endogenous control, we used the Mus-F (5′-GCAAAGCCTGACAACTTCTGAA-3′) and Mus-R (5′-CCAACGTCCCAGCTTAAGTAGAAT-3′) primers coupled with the MM-1 probe (5′-HEX-AAAGCATCTGCCTCCG-BHQ-1-3′) to amplify a 67-bp *Mus musculus* GAPDH sequence. The primers and probes were designed using Primer Express 3.0 Software (Applied Biosystems, USA) and manufactured by Integrated DNA Technologies (Coralville, IA, USA). The PCR reactions were performed using an ABI 7300 real-time thermocycler (Applied Biosystems, USA). The reaction mixture had a final volume of 20 μL and contained 10 ng of genomic DNA, 4 μL of HOT FIREPol Probe qPCR Mix Plus (Solis BioDyne, Tallinn, Estonia), 200 nM of each primer, and 100 nM of the TcSt-1 probe or 200 nM of the MM-1 probe. ROX was used as a reference dye. For both TaqMan assays, the thermal cycle consisted of a polymerase activation step carried out at 95 °C for 10 min (one cycle) and a two-step amplification phase: 95 °C for 15 s and 55 °C for 45 s (40 cycles). Fluorescence was measured at the end of each amplification cycle. The data were analyzed using a 7300 System SDS software with the SDS relative quantitation plug-in (Applied Biosystems, USA). All data were analyzed by the $2^{-\Delta\Delta CT}$ method (Livak and Schmittgen, 2001), comparing the C_Ts of the *T. cruzi* gene versus that of GAPDH as well as comparing all of the samples with the control. The parasite load is expressed as the relative DNA load compared with the control.

2.9. Cardiac histopathological analysis

Hearts were extracted at the moment of death from mice that died before the end point. Surviving mice were euthanized at 18 dpi and their hearts were also extracted. Hearts were longitudinally sectioned for further analysis by histopathology and qPCR. Samples were fixed in 10% formaldehyde 0.1 M phosphate buffer (pH 7.3) for 24 h, dehydrated in alcohol, clarified in xylene, and embedded in paraffin. 5 μm sections were obtained and stained with hematoxylin-eosin for routine histopathological analysis as well as to evaluate the presence of *T. cruzi* amastigote nests and inflammation of the myocardium (Duaso et al., 2010; Faundez et al., 2008). Amastigote nests were counted using the ImageJ Software (ver. 1.46), using the “cell counter” tool, to avoid duplication of nests counted. For each quantification we considered at least five nonconsecutive slides of tissue from six different mice.

2.10. Thiol content in T. cruzi epimastigotes

Thiol content was measured as we previously described (Faundez et al., 2005; Maya et al., 1997). Parasites were cultured in PBS with D-Glucose (5 g/L) for 24 h at 27 °C, to deplete $T(SH)_2$ content. After that, putrescine (50 μM) and glutathione methyl-ester (GSH-MEE, 100 μM) were added to let the parasites recover from $T(SH)_2$ production. Pentamidine (50 and 100 μM) was added at the same time as putrescine. After 6 h of incubation at 27 °C, parasites were harvested, and the thiol content was measured as follows: epimastigotes, equivalent to 1 mg of protein were suspended in 40 mM HEPES–2 mM EDTA buffer (pH 8) with 2 mM monobromobimane and incubated at 70 °C for 5 min. To precipitate proteins, 4 M methanesulfonic acid was added. After 10 min of incubation at 4 °C, the sample was centrifuged at 10,000 *g* for 3 min and the supernatant was filtered using a Millex® syringe driven filter unit with 0.22 μm filter pore (Millipore, USA). A 20 μL sample was injected on a Gemini C18 (5 μm) reverse-phase column (Phenomenex, USA), and eluted for 60 min at a flow rate of 1 mL/min. The elution gradient was as follows: 0–20 min, 90% solvent A (0.25% [wt/vol] lithium-camphorsulfonate, pH 2.35) and 10% solvent B (25% [wt/vol] 1-propanol in solution A); 20–40 min, linear gradient of 10–50% solvent B; 40–60 min, 50% solvent B isocratic in solvent A, returning to the initial conditions in 30 min. All measurements were performed with a Merck-Hitachi L-6200 Intelligent Pump high-pressure chromatograph with an F-1050 fluorescence detector and a D-2500 integrator. Emission and excitation wavelengths were 480 and 385 nm, respectively. This method detects reduced free thiols but not disulfides.

2.11. Radiolabeled molecules transport assays

Aliquots of *T. cruzi* (Y strain) epimastigote cells (10^7 parasites) were centrifuged at 8000*g* for 30 s and washed once with phosphate-buffered saline supplemented with 2% [wt/vol] glucose (PBS-G). The cells were then resuspended in 0.2 mL of PBS-G containing 5 μM [^{14}C]-putrescine (NEN/DuPont, Boston, MA, USA; 0.4 μCi) or [^{3}H]-Thymidine (Perkin Elmer, Waltham, MA, USA; 1 mCi/mL). Following incubation for 5 min at 28 °C, the cells were centrifuged at 8000*g* for 30 s and washed twice with 1 mL of ice-cold PBS-G. The pellets were then resuspended and radioactivity was assessed using an UltimaGold XR liquid scintillation cocktail (Perkin Elmer, USA). Non-specific transport and carry over were measured in transport mixtures containing 10 mM putrescine (Pereira et al., 1999). All assays were run at least in triplicate.

2.12. Statistical analysis

For the combination experiments, the data was analyzed using the COMBENEFIT free software (Di Veroli et al., 2016). All other statistical analyses were performed using GraphPad Prism (6.0) software. For all experiments, the statistical significance was established at $p < 0.05$. Normal distribution of data was assessed using D'Agostino-Pearsons analysis. One-way or Two-way ANOVA (with Tukey or Bonferroni post-test) or *t*-test analysis were performed when required. For survival analysis, the log-rank (Mantel Cox) test was performed.

3. Results

3.1. Pentamidine antagonizes the effect of benznidazole in isolated trypomastigotes

To study the outcome of the BNZ + PTM combination, we performed a dose-matrix approach, comparing the effect of the combination between 8 concentrations of PTM and 8 concentrations of BZN in a 2-fold dilution scheme. We analyzed the data using the free software COMBNENEFIT (Di Veroli et al., 2016). We choose the Bliss independence approach for the data analyzes, assuming that both drugs have different action mechanisms (Fitzgerald et al., 2006; Foucquier and Guedj, 2015). The results are shown in the Fig. 1. Fig. 1A and B illustrate the effect of PTM and BNZ, respectively, showing that the absolute EC_{50} (the concentration that decreases the viability of parasites in a 50%) is 12.2 μM for PTM and 40.8 μM for BNZ. The dose-matrix combination (Fig. 1C) shows the combination modeling between PTM and BNZ by using the Bliss Independence model. When we compared the real-data registered by each combination point, the synergy heatmaps (Fig. 1C, lower panels) are obtained. The synergy heatmaps show an antagonistic behavior at middle-high concentrations of BNZ and low concentrations of PTM. The orange/red quadrants in the dose-matrix graph, and the high and red areas in the surface model, indicate antagonistic significance between the data obtained and the Bliss model performed by the software. No one synergistic point was detected at any point of the combinations.

3.2. Pentamidine antagonizes the effect of benznidazole in an in vitro model of infection

We studied the influence of PTM on the effect of BNZ in an *in vitro* model of infection. We infected RAW 264.7 cells, and measured the parasite load by qPCR after treatments. We used two low-effective concentrations of PTM (0.5 and 1 μM). In our current model, PTM alone at these concentrations does not modify the parasite load in infected cells (data not shown).

As Fig. 2 shows, BNZ showed a concentration-dependent effect, decreasing the parasite load by 40, 60 and 90% at 1, 2 or 10 μM, respectively. When we combined BNZ with two concentration of PTM (0.5 and 1 μM), we found that PTM reversed the effect of BNZ mainly at 0.5 μM of PTM. A two-way analysis of the effect of each concentration of PTM over the effect of BNZ indicated that the addition of 0.5 μM PTM significantly modified the effect of BNZ ($p = 0.012$). However, PTM at 1 μM only showed a trend towards antagonism, but without statistical significance ($p = 0.072$).

3.3. Pentamidine lacks of synergism with benznidazole in mice infected with T. cruzi

We assessed the influence of PTM on BNZ treatment used at two different doses (5 and 20 mg/kg/day). As expected, BNZ had a dose-dependent effect, increasing the median survival from 14 to 17 days at 5 mg/kg/day, and getting an undefined median survival at 20 mg/kg/day. We combined both doses of BNZ with an ineffective dose of PTM (4 mg/kg) (Diaz et al., 2014). Unexpectedly, mice treated with BNZ (5 mg/kg) together with PTM (4 mg/kg) had a median survival shorter than those treated with BNZ 5 mg/kg alone (BNZ 5 + PTM: 15 days, BNZ 5: 17 days), reaching the same median survival than the untreated control (15 days) control, but without statistical difference when compared with BNZ 5 mg/kg alone ($p = 0.55$). On the other hand, when we combined PTM with the high dose of BNZ (20 mg/kg), we found that the outcome was largely influenced by the effect of BNZ, without significant changes on the survival induced by PTM (Fig. 3A).

Alternatively, the combination of PTM with 5 mg/kg BNZ had an antagonistic behavior over the parasite load in murine blood. In this setting, 5 mg/kg BNZ provoked a decrease of parasitemia, which was reversed significant by the addition of PTM (Fig. 3B). In contrast, the addition of PTM did not modify the effect of 20 mg/kg BNZ, being both significantly lower than the control (Fig. 3C).

We also analyzed heart structure in the infected and treated

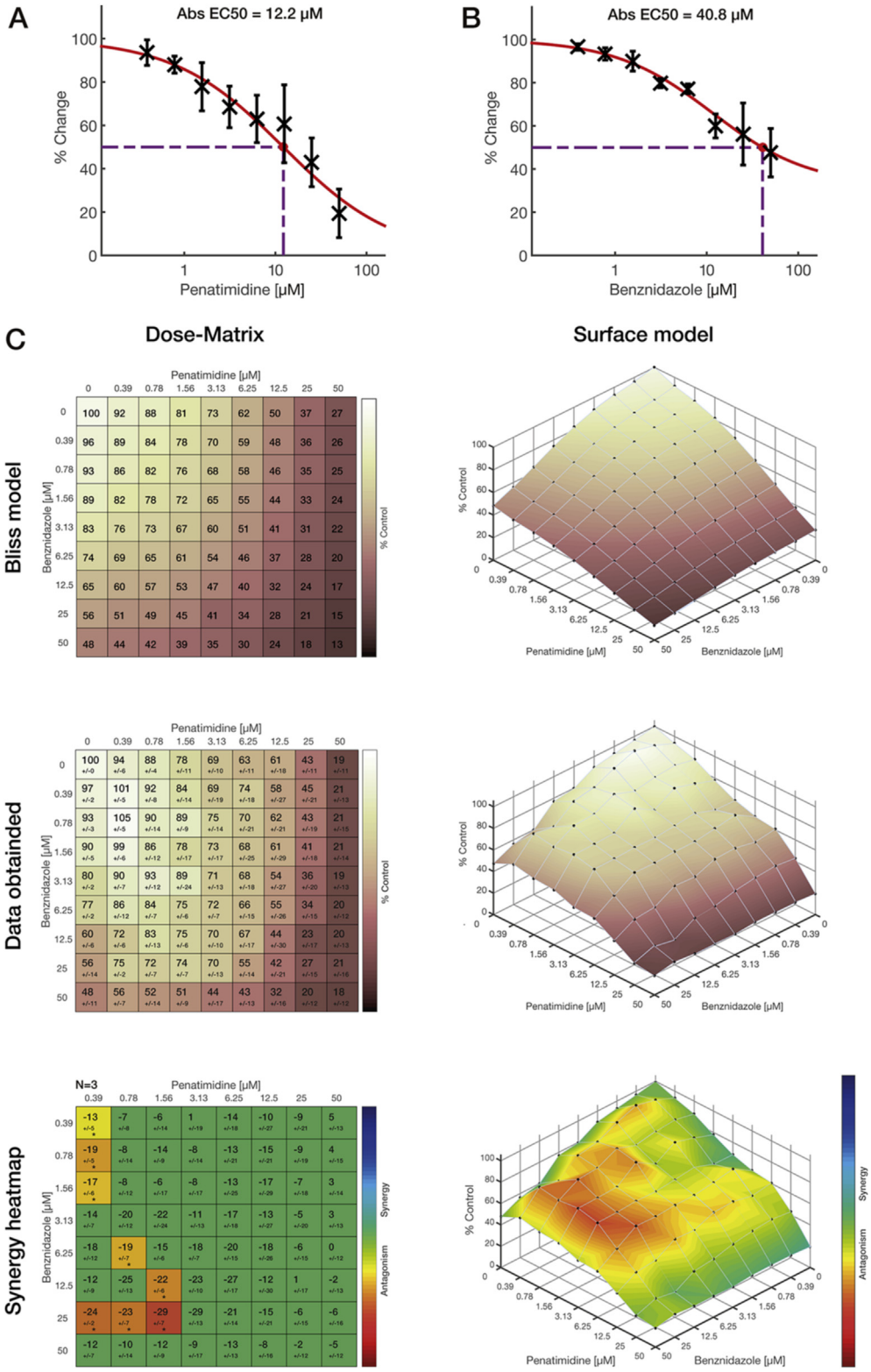

Fig. 1. Effect of benznidazole (BNZ), pentamidine (PTM) and their combination in isolated trypomastigotes of *T. cruzi*. Isolated trypomastigotes of *T. cruzi* (Y strain) were seeded in 96-well plates (10^6 parasites per well) and exposer for 24 h to PTM, BNZ and their combinations. Cell viability was measured by MTT reduction. **A**. Dose-response curve for the effect of PTM on the cell viability. **B**. Dose-response curve for the effect of BNZ on the cell viability. **C**. Study of the combination between PTM and BNZ in a dose-matrix and surface model view. The combination data was analyzed using the Bliss Independence model. The uppers panels show the Bliss model assuming no interaction (additivity) between drugs, based in the activities registered by each drug alone (panles A and B). Middle panels show the real-data obtained when the drugs were combined. Lower panels shows the difference between the real data and the Bliss model, this difference is expressed as a synergy heatmap. The dose-matrix heatmap shows the synergy score for each combination. Negative values represent an antagonistic combination. The combinations with statistical significance are colored, the non-significant values are showed in green. The heatmap in the XYZ model shows in red color the areas in which the combination results antagonistic. $^*p < 0.05$. The data is expressed as the mean of three independent experiments. (For interpretation of the references to colour in this figure legend, the reader is referred to the web version of this article.)

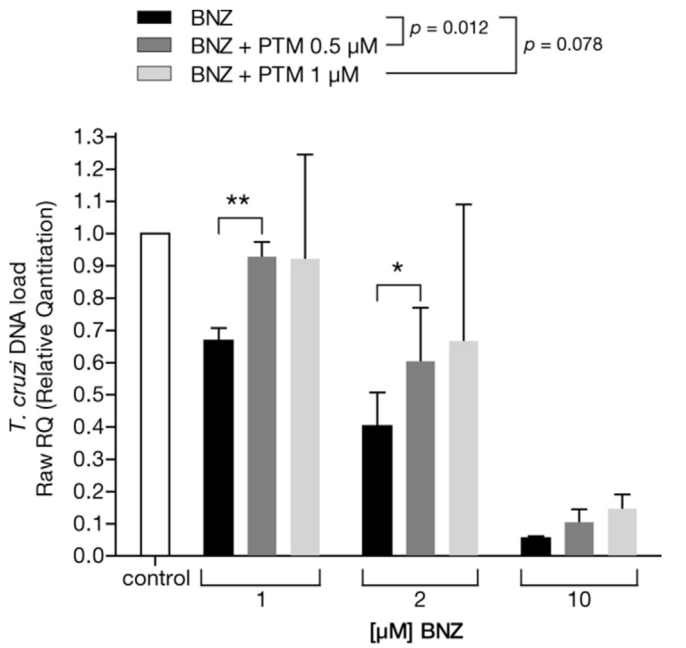

Fig. 2. Effect of the combination between BNZ and PTM in infected cells. RAW 264.7 cells were infected with trypomastigotes of *T. cruzi* (Y strain) for 24 h, and were then treated with BNZ, PTM or BNZ + PTM at the concentrations indicated in the figure, for 48 h. Then, DNA was isolated and the parasite load was quantified by qPCR amplification. Graph data is expressed as the mean ± SD of three independent experiments. *p* values indicated in the figure legend show the significance between the effect of the treatment with BNZ alone or in the presence of PTM (0.5 or 1 μM), calculated by 2-way ANOVA, whereas the difference between the indicated bars, was calculated by two-way ANOVA plus Bonferroni post-test of multiple comparisons. For all comparisons, *: $p < 0.05$, **: $p < 0.01$.

mice, by routine histology. Fig. 3 shows that only 20 mg/kg BNZ was able to reduce the inflammatory infiltrate, a phenomenon that was not reverted by the addition of PTM. The treatment with 5 mg/kg BNZ, with or without PTM, did not induce changes in the inflammatory state of myocardium (Fig. 4A). When we quantified the number of amastigote nests from these hearts, we found that BNZ at 5 and 20 mg/kg induced a significant decrease in the amastigote nest number. PTM induced a slight (but not significant) reversion on the effect of 5 mg/kg BNZ. On the other hand, PTM did not modify the effect of 20 mg/kg BNZ (Fig. 4B). To further study the parasite load in heart tissue from infected and treated mice, we carried out a qPCR quantitation (Fig. 4C). qPCR quantitation showed that PTM did not modify the effect of 5 and 20 mg/kg BNZ.

3.4. Pentamidine does not modify trypanothione levels in T. cruzi epimastigotes

Even though the mode of action of BNZ is not entirely clear yet, there is strong evidence suggesting the important role of $T(SH)_2$ in the resistance of *T. cruzi* against BNZ, revealed by the decrease of free $T(SH)_2$ after epimastigote exposure to BNZ (Trochine et al., 2014) and the increase of the BNZ affect after the GSH (and $T(SH)_2$, consequently) synthesis inhibition (Faundez et al., 2005). We previously showed that PTM blocks putrescine and spermidine transport in *T. cruzi* (Diaz et al., 2014), hypothesizing that this blockade induces $T(SH)_2$ depletion in *T. cruzi*, modifying the resistance against BNZ. Due to the lack of synergism, we analyzed $T(SH)_2$ levels in epimastigotes exposed to PTM 10 μM (Fig. 5). Parasites were depleted of $T(SH)_2$ by incubating in PBS and Glucose for 24 h. Next, parasite culture was supplemented with putrescine 50 μM and glutathione methyl-ester (GSH-MEE, 100 μM), to make $T(SH)_2$

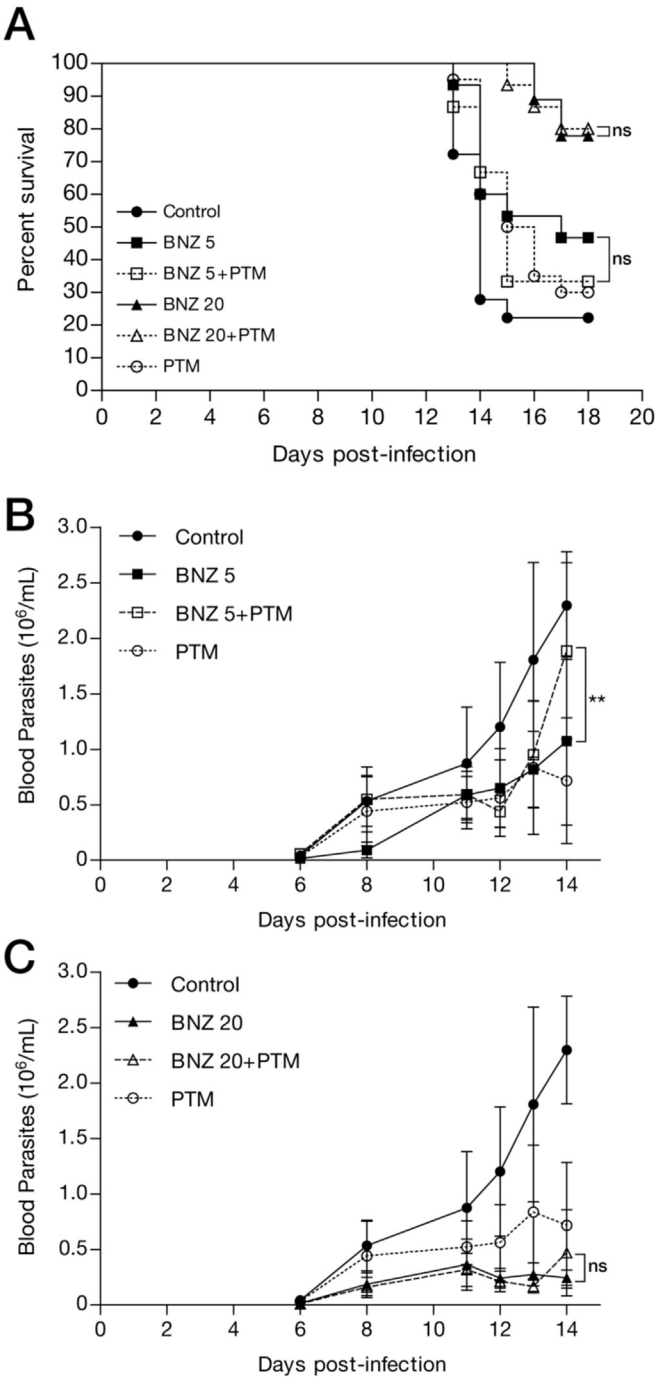

Fig. 3. Effect of benznidazole (BNZ), pentamidine (PTM) and their combination in the survival and parasitemia of *T. cruzi*-infected mice. BALB/c mice were infected with *T. cruzi* trypomastigotes (Y strain) and treated with BNZ (5 or 20 mg/kg/day, by oral route), PTM (4 mg/kg/day, intraperitoneal) and their combination, for 15 days. **A.** Survival rates of infected and treated mice. Survival was recorded daily, until day 18 post-infection. The graph summarizes two independent experiments with n = 6 each. All statistical comparisons between groups were calculated by log-rank (Mantel Cox) test. **B.** Parasitemia of infected mice (n = 6) treated BNZ 5 mg/kg, PTM (4 mg/kg), and their combination by 15 days. **C.** Parasitemia of infected mice (n = 6) treated with BNZ 20 mg/kg, PTM (4 mg/kg), and their combination by 15 days. For panels B and C, the bars indicate the standard deviation of the means. The asterisks indicate the significance between groups at day 14 post infection. **: $p < 0.001$, **ns**: non-significant, calculated by two-way ANOVA and Bonferroni post-test.

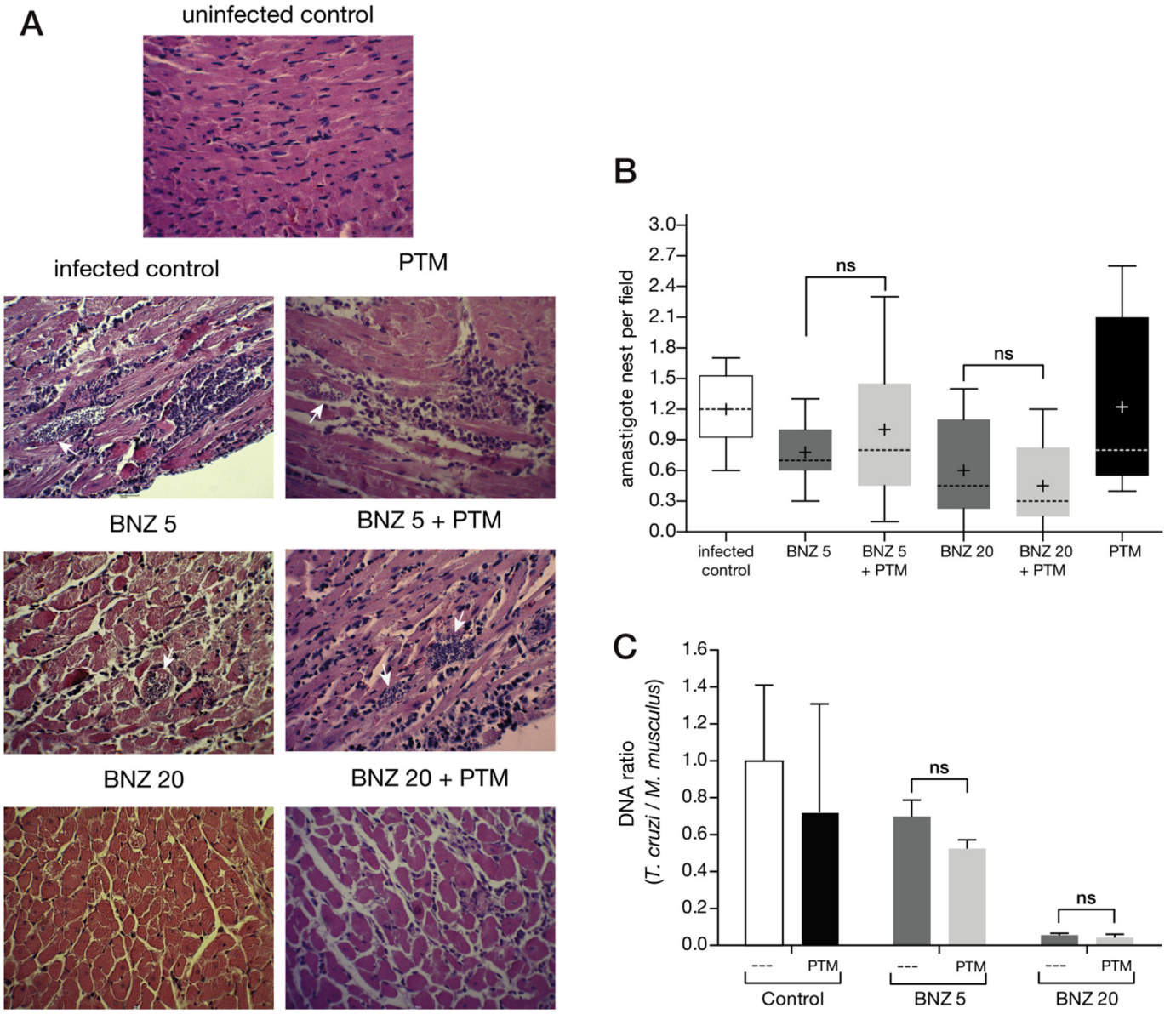

Fig. 4. Effect of benznidazole (BNZ), pentamidine (PTM) and their combination in the inflammation and amastigote load in *T. cruzi*-infected mice. BALB/c mice were infected with *T. cruzi* trypomastigotes (Y strain) and treated with BNZ (5 or 20 mg/kg/day, by oral route), PTM (4 mg/kg/day, intraperitoneal) and their combination, for 15 days. **A**. Histopathology of infected BALB/c mice with or without treatment at 18 days post-infection. The sections were stained with hematoxilyn and eosin. The white arrowheads indicate amastigote nests. The images are representative of at least 5 mice in each group with similar results. **B**. Quantitation of amastigote nest of heart sections from infected mice. The graph summarizes the quantitation of at least 4 mice per group, from 2 independent experiments. Data are expressed as mean (plus sign), median (discontinuous line), 95% confidence interval (box) and SD. Statistical comparisons were performed by unpaired *t*-test. **ns**: no significant differences between groups. **C**. Effect of BNZ, PTM, and their combination in the DNA parasite load in hearts from *T. cruzi*-infected mice. Hearts from mice were extracted on the day of death or on day 18 for survivors. The graph data are expressed as the means ± SD of 6 mice per group. **ns**: no significant differences between groups, calculated by two-way ANOVA and Bonferroni post-test.

synthesis independent of glutathione synthesis. As expected, addition of putrescine and exogenous GSH-MEE restored the levels of $T(SH)_2$ in depleted parasites, whereas the GSH were not altered. PTM did not affect $T(SH)_2$ levels, even at high concentrations such as 50 μM. These data indicate that even though there is a competition for the transport system (Diaz et al., 2014), it was unable to induce a significant decrease in $T(SH)_2$ levels, thus, the action mechanism and the antagonism provoked by PTM should respond to another mode of action.

3.5. The effect of PTM does not correlate with its ability to block putrescine transport

Finally, to further explore the relationship between the blockade of putrescine transport by PTM and the effect of the drug over the parasite viability, we overexpressed the TcPAT12 permease (also called TcPOT1.1/1.2), the protein responsible for putrescine transport in the parasite (Carrillo et al., 2006; Hasne et al., 2010; Soysa et al., 2013). . As Fig. 6A shows, in epimastigotes overexpressing TcPAT12, putrescine uptake increased by two fold, compared with control parasites overexpressing the green fluorescent protein (GFP: 0.30 ± 0.03, TcPAT12: 0.81 ± 0.09 pmol/(min × 10^7 cells)). As expected, in both parasite groups (TcPAT12 and GFP), PTM 50 μM blocked putrescine uptake in at least 80% (GFP: 0.05 ± 0.01, TcPAT12: 0.11 ± 0.03 pmol/(min × 10^7 cells)). As control, we measured the transport of radiolabeled thymidine, which was not affected by 50 μM PTM (Thymidine = 4.59 ± 0.66% pmol/(min × 10^7 cells), Thymidine + PTM = 5.29 ± 0.50 pmol/

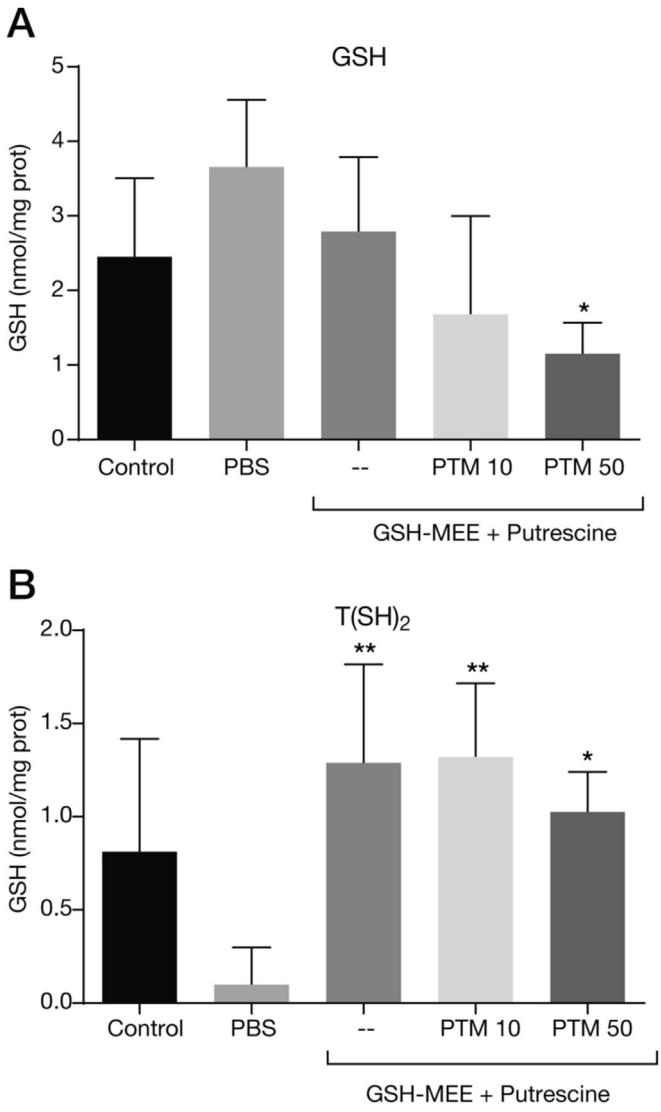

Fig. 5. Effect of pentamidine (PTM) in the trypanothione ($T(SH)_2$) content of *T. cruzi* epimastigotes. Epimastigotes of *T. cruzi* (Y strain) were placed in phosphate-saline buffer with glucose (PBS) for 24 h, and were then supplemented with glutathione monoethyl-ester (GSH-MEE, 100 μM) and putrescine (50 μM), for 6 h to recover $T(SH)_2$ levels. Parasites were also treated with PTM 10 or 50 μM, to evaluate the relationship between putrescine transport and $T(SH)_2$ levels. Parasites were then harvested, and the content of: **A**. GSH or, **B**. $T(SH)_2$ was measured by HPLC. In both panels, the thiol levels are expressed as nmol of: GSH per mg of protein. *: $p < 0.05$, **: $p < 0.01$, compared with the PBS control group, calculated with one-way ANOVA and Tukey's post-test.

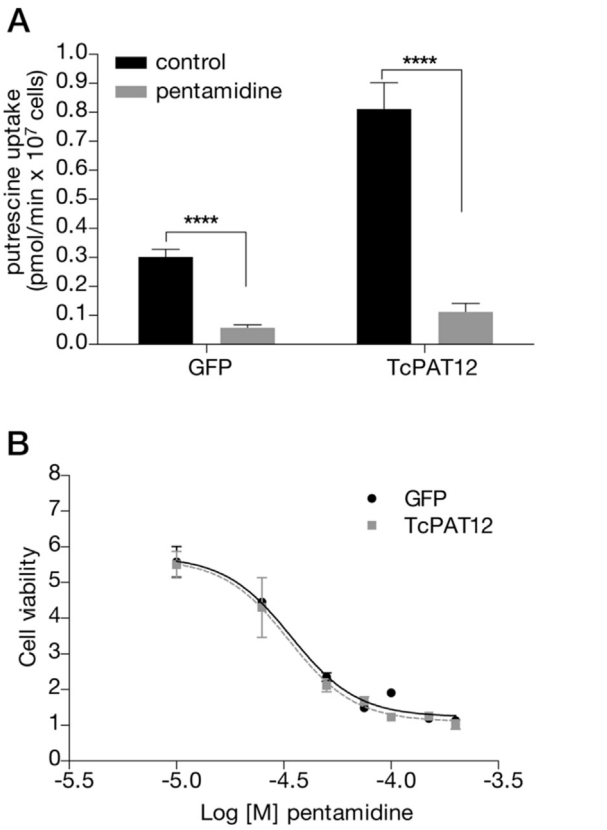

Fig. 6. Effect of pentamidine (PTM) on the putrescine uptake and viability of *T. cruzi* epimastigotes overexpressing the TcPAT12 transporter. Epimastigotes of *T. cruzi* (Y strain) were transfected with pTREX-TcPAT12 and pTREX-GFP as a control A. Transport of [^{14}C]-putrescine (5 μM) was measured at 10 min in the absence or presence of PTM at a 10-fold excess. The results are expressed as the mean ± SD of triplicate experiments. ****: $p < 0.0001$; compared to its respective controls without pentamidine, calculated using a Two-way ANOVA and Bonferroni post-test. Transport of putrescine was found to increase linearly with time (initial velocities) up to 30 min. B. Viability analysis of GFP-transfected and TcPAT12 overexpressing parasites treated with PTM. EC_{50} values for GFP-transfected parasites were 34.2 μM and 33.5 μM in TcPAT12 transfected parasites. Viability assays were performed by direct microscopic examination.

(min × 10^7 cells). In addition, we previously reported that PTM (50 μM) does not affect the transport of L-arginine and L-aspartate (Diaz et al., 2014). When we analyzed the effect of PTM on parasite viability, we found that PTM had the same effect in both parasite models, with EC_{50} values of 34.2 μM in GFP and 33.5 μM in TcPAT12 transfected parasites (Fig. 6B). These results agree with the $T(SH)_2$ data showed in Fig. 5, and support the idea that putrescine transport, and the consequent alteration of $T(SH)_2$ synthesis is not the main target of PTM.

4. Discussion

Polyamine metabolism has been studied as a way to improve the effect of drugs against some parasites such as *Trypanosoma brucei (T. brucei)*. Indeed, the combination of nifurtimox and eflornithine (an inhibitor of putrescine synthesis), also called NECT (nifurtimox-eflonithine combination therapy) is included in the Essential Medicines List of the WHO since 2009 (Yun et al., 2010), and its safety compared with other treatments seems to be its greatest advantage (Eperon et al., 2014). However, basic studies failed to find a synergistic effect between these drugs in isolated *T. brucei* parasites (Vincent et al., 2012). In this setting, the results reported by Vincent et al. agree with our data, given that a decrease in putrescine synthesis by DFMO did not reduce trypanothione levels. We previously showed that PTM competitively blocks the transport of putrescine in *T cruzi*, the only trypanosomatid unable to synthetize putrescine (Diaz et al., 2014), but it did not modify $T(SH)_2$ levels in the parasite (Fig. 5).

On the other hand, as Fig. 6 shows, despite the strong blocking effect of PTM, concentrations as large as 50 μM were not able to completely inhibit putrescine uptake. Thus, it is possible that other transporters of diamines could also mediate the uptake of putrescine. Indeed, in addition to TcPAT12, there are 5 genomic sequences that correlate with putative polyamine transporters (Reigada et al., 2016). So, these low levels of putrescine uptake could be enough to maintain the $T(SH)_2$ in adequate levels (Fig. 6). It was also described that TcPAT12 mediates the uptake of spermidine (Carrillo et al.,

2006), which is also blocked by PTM (Diaz et al., 2014), but, similar to putrescine uptake, this blockade might not be able to completely deplete the spermidine content of the parasites.

It is common that key cellular functions have redundant or overexpressed pathways to ensure the levels of essential compounds. $T(SH)_2$ is an example of that. For instance, the enzyme that regulates the levels of reduced trypanothione, trypanothione reductase (TcTryR), has a high natural abundance in *T. cruzi* and has a large *Ki*. Consequently, to have a real depletion of reduced $T(SH)_2$ (its functional form), the enzyme must be inhibited by more than 98% (Olin-Sandoval et al., 2012). Thus, it is reasonable to think that putrescine transport has a similar pattern of redundancy to ensure stable $T(SH)_2$ levels.

PTM itself has also been proved to potentiate other antimicrobial drugs. Indeed, a high-throughput screening in the fungus *Saccharomyces cerevisiae*, where PTM was classified as a 'promiscuous synergic' drug, but this effect was linked to the ability of PTM to inhibit the mitochondrial protein Pnt1, present in yeast but not in trypanosomatids (according to the genome data) (Cokol et al., 2011). PTM has also been assayed to potentiate trypanocidal drugs *in vivo*. Jeganathan et al. (2011) also found a synergistic effect between PTM and nifurtimox in experimental African trypanosomiasis (HAT), but this effect is due to an alteration of the pharmacokinetics of nifurtimox in the presence of PTM. Specifically, PTM increases the crossing of nifurtimox through the blood-brain barrier (BBB) (Jeganathan et al., 2011). This could be an advantage for the treatment of HAT, because nifurtimox must pass through the BBB to affect the parasites causing the disease. In our case, given that Chagas disease is a systemic peripheral illness, this kind of pharmacokinetic interaction is not specifically beneficial for treatment.

5. Conclusions

We found that pentamidine antagonizes the effect of benznidazole *in vitro*, and fails synergize with benznidazole *in vivo*. In addition, we explored the association between the effect of pentamidine, the transport of putrescine and the trypanothione levels. We found that pentamidine did not induce a depletion of $T(SH)_2$. Also, in parasites that overexpress the putrescine permease TcPAT12, pentamidine killing ability was not decreased. Our results suggest that, regardless of the ability to blockade the putrescine transport, the TcPAT12 permease is not the main target of pentamidine effect, and could explain the lacking of synergism between that drug and benznidazole.

Acknowledgements

This work was supported by grants from the Consejo Nacional de Ciencia y Tecnología (CONICYT-Chile, http://www.conicyt.cl/), grants FONDECYT: 11110182 and 1160807 (RLM), 1120230 (UK) and 1130189 (JDM); Vicerrectoría de Investigación y Desarrollo, Universidad de Chile (http://www.uchile.cl/investigacion), grant U-INICIA 11/07 (RLM); Consejo Nacional de Investigaciones Científicas y Técnicas (CONICET, PIP. http://www.conicet.gov.ar), grants 2010-0685 (CAP) and 2011-0263 (MRM), Agencia Nacional de Promoción Científica y Tecnológica (FONCYT, PICT. http://www.agencia.mincyt.gob.ar) grants 2012-0559 (CAP) and 2013-2218 (MRM). M.R.M. and C.A.P are members of the career of scientific investigator of CONICET (Argentina). The funders had no role in study design, data collection and analysis, decision to publish, or preparation of the manuscript.

References

Camargo, E.P., 1964. Growth and differentiation in trypanosoma cruzi. I. Origin of metacyclic trypanosomes in liquid media. Rev. Inst. Med. Trop. Sao Paulo 6, 93–100.
Carrillo, C., Canepa, G.E., Algranati, I.D., Pereira, C.A., 2006. Molecular and functional characterization of a spermidine transporter (TcPAT12) from Trypanosoma cruzi. Biochem. Biophys. Res. Commun. 344, 936–940.
Cokol, M., Chua, H.N., Tasan, M., Mutlu, B., Weinstein, Z.B., Suzuki, Y., Nergiz, M.E., Costanzo, M., Baryshnikova, A., Giaever, G., Nislow, C., Myers, C.L., Andrews, B.J., Boone, C., Roth, F.P., 2011. Systematic exploration of synergistic drug pairs. Mol. Syst. Biol. 7, 544.
Chagas, C., 1909. Nova tripanosomiase humana. Estudios sobre a morfología e o ciclo evolutivo do Schizotrypanum cruzi n.gen, n.sp., agente etiológico do nova entidae mórbida do homen. Mem. Inst. Oswaldo Cruz 1, 159–218.
Di Veroli, G.Y., Fornari, C., Wang, D., Mollard, S., Bramhall, J.L., Richards, F.M., Jodrell, D.I., 2016. Combenefit: an interactive platform for the analysis and visualization of drug combinations. Bioinformatics 32 (18), 2866–2868.
Díaz-Urrutia, C.A., Olea-Azar, C.A., Zapata, G.A., Lapier, M., Mura, F., Aguilera-Venegas, B., Arán, V.J., López-Múñoz, R.A., Maya, J.D., 2012. Biological and chemical study of fused tri- and tetracyclic indazoles and analogues with important antiparasitic activity. Spectrochim. Acta A 95, 670–678.
Diaz, M.V., Miranda, M.R., Campos-Estrada, C., Reigada, C., Maya, J.D., Pereira, C.A., Lopez-Munoz, R., 2014. Pentamidine exerts in vitro and in vivo anti Trypanosoma cruzi activity and inhibits the polyamine transport in Trypanosoma cruzi. Acta Trop. 134, 1–9.
Duaso, J., Rojo, G., Cabrera, G., Galanti, N., Bosco, C., Maya, J.D., Morello, A., Kemmerling, U., 2010. Trypanosoma cruzi induces tissue disorganization and destruction of chorionic villi in an ex vivo infection model of human placenta. Placenta 31, 705–711.
Eperon, G., Balasegaram, M., Potet, J., Mowbray, C., Valverde, O., Chappuis, F., 2014. Treatment options for second-stage gambiense human African trypanosomiasis. Expert Rev. Anti Infect. Ther. 12, 1407–1417.
Fairlamb, A., Blackburn, P., Ulrich, P., Chait, B., Cerami, A., 1985. Trypanothione: a novel bis(glutathionyl)spermidine cofactor for glutathione reductase in trypanosomatids. Science 227, 1485–1487.
Faundez, M., Lopez-Munoz, R., Torres, G., Morello, A., Ferreira, J., Kemmerling, U., Orellana, M., Maya, J.D., 2008. Buthionine sulfoximine has anti-Trypanosoma cruzi activity in a murine model of acute Chagas' disease and enhances the efficacy of nifurtimox. Antimicrob. Agents Chemother. 52, 1837–1839.
Faundez, M., Pino, L., Letelier, P., Ortiz, C., Lopez, R., Seguel, C., Ferreira, J., Pavani, M., Morello, A., Maya, J.D., 2005. Buthionine sulfoximine increases the toxicity of nifurtimox and benznidazole to Trypanosoma cruzi. Antimicrob. Agents Chemother. 49, 126–130.
Fitzgerald, J.B., Schoeberl, B., Nielsen, U.B., Sorger, P.K., 2006. Systems biology and combination therapy in the quest for clinical efficacy. Nat. Chem. Biol. 2, 458–466.
Foucquier, J., Guedj, M., 2015. Analysis of drug combinations: current methodological landscape. Pharmacol. Res. Perspect. 3, e00149.
Hall, B.S., Wilkinson, S.R., 2012. Activation of benznidazole by trypanosomal type I nitroreductases results in glyoxal formation. Antimicrob. Agents Chemother. 56, 115–123.
Hasne, M.P., Coppens, I., Soysa, R., Ullman, B., 2010. A high-affinity putrescine-cadaverine transporter from Trypanosoma cruzi. Mol. Microbiol. 76, 78–91.
Jeganathan, S., Sanderson, L., Dogruel, M., Rodgers, J., Croft, S., Thomas, S.A., 2011. The distribution of nifurtimox across the healthy and trypanosome-infected murine blood-brain and blood-cerebrospinal fluid barriers. J. Pharmacol. Exp. Ther. 336, 506–515.
Livak, K.J., Schmittgen, T.D., 2001. Analysis of relative gene expression data using real-time quantitative PCR and the 2(-Delta Delta C(T)) Method. Methods 25, 402–408.
Manta, B., Comini, M., Medeiros, A., Hugo, M., Trujillo, M., Radi, R., 2013. Trypanothione: a unique bis-glutathionyl derivative in trypanosomatids. Biochem. Biophys. Acta 1830 (5), 3199–3216.
Maya, J.D., Repetto, Y., Agosin, M., Ojeda, J.M., Tellez, R., Gaule, C., Morello, A., 1997. Effects of nifurtimox and benznidazole upon glutathione and trypanothione content in epimastigote, trypomastigote and amastigote forms of Trypanosoma cruzi. Mol. Biochem. Parasitol. 86, 101–106.
Mejia, A.M., Hall, B.S., Taylor, M.C., Gomez-Palacio, A., Wilkinson, S.R., Triana-Chavez, O., Kelly, J.M., 2012. Benznidazole-resistance in Trypanosoma cruzi is a readily acquired trait that can arise independently in a single population. J. Infect. Dis. 206, 220–228.
Molina-Berríos, A., Campos-Estrada, C., Henriquez, N., Faúndez, M., Torres, G., Castillo, C., Escanilla, S., Kemmerling, U., Morello, A., López-Muñoz, R.A., Maya, J.D., 2013a. Protective role of acetylsalicylic acid in experimental trypanosoma cruzi infection: evidence of a 15-epi-Lipoxin A4-mediated effect. PLoS Negl. Trop. D. 7, e2173.
Molina-Berrios, A., Campos-Estrada, C., Lapier, M., Duaso, J., Kemmerling, U., Galanti, N., Ferreira, J., Morello, A., Lopez-Munoz, R., Maya, J.D., 2013b. Protection of vascular endothelium by aspirin in a murine model of chronic Chagas' disease. Parasitol. Res. 112, 2731–2739.
Molina-Berrios, A., Campos-Estrada, C., Lapier, M., Duaso, J., Kemmerling, U., Galanti, N., Leiva, M., Ferreira, J., Lopez-Munoz, R., Maya, J.D., 2013c. Benznidazole prevents endothelial damage in an experimental model of Chagas

disease. Acta Trop. 127, 6–13.
Morillo, C.A., Marin-Neto, J.A., Avezum, A., Sosa-Estani, S., Rassi Jr., A., Rosas, F., Villena, E., Quiroz, R., Bonilla, R., Britto, C., Guhl, F., Velazquez, E., Bonilla, L., Meeks, B., Rao-Melacini, P., Pogue, J., Mattos, A., Lazdins, J., Rassi, A., Connolly, S.J., Yusuf, S., Investigators, B., 2015. Randomized trial of benznidazole for chronic Chagas' cardiomyopathy. N. Engl. J. Med. 373, 1295–1306.
Mosmann, T., 1983. Rapid colorimetric assay for cellular growth and survival: application to proliferation and cytotoxicity assays. J. Immunol. Methods 65, 55–63.
National Research Council (U.S.) Committee for the Update of the Guide for the Care and Use of Laboratory Animals, Institute for Laboratory Animal Research (U.S.), and National Academies Press (U.S.), 2011. Guide for the Care and Use of Laboratory Animals. National Academies Press, Washington, D.C.
Olin-Sandoval, V., Gonzalez-Chavez, Z., Berzunza-Cruz, M., Martinez, I., Jasso-Chavez, R., Becker, I., Espinoza, B., Moreno-Sanchez, R., Saavedra, E., 2012. Drug target validation of the trypanothione pathway enzymes through metabolic modelling. FEBS J. 279, 1811–1833.
Pereira, C.A., Alonso, G.D., Paveto, M.C., Flawia, M.M., Torres, H.N., 1999. L-arginine uptake and L-phosphoarginine synthesis in Trypanosoma cruzi. J. Eukaryot. Microbiol. 46, 566–570.
Reigada, C., Saye, M., Vera, E.V., Balcazar, D., Fraccaroli, L., Carrillo, C., Miranda, M.R., Pereira, C.A., 2016. Trypanosoma cruzi polyamine transporter: its role on parasite growth and survival under stress conditions. J. Membr. Biol. 249, 475–481.
Riarte, A., TRAENA: Placebo-controlled evaluation of impact of benznidazole treatment on long-term disease progression in adults with chronic Chagas disease. 62nd Annual Meeting of the American Society of Tropical Medicine and Hygiene, Washington, DC, USA., 2013.
Soysa, R., Venselaar, H., Poston, J., Ullman, B., Hasne, M.P., 2013. Structural model of a putrescine-cadaverine permease from Trypanosoma cruzi predicts residues vital for transport and ligand binding. Biochem. J. 452, 423–432.
Trochine, A., Creek, D.J., Faral-Tello, P., Barrett, M.P., Robello, C., 2014. Benznidazole biotransformation and multiple targets in Trypanosoma cruzi revealed by metabolomics. PLoS Negl. Trop. Dis. 8, e2844.
Vazquez, M.P., Levin, M.J., 1999. Functional analysis of the intergenic regions of TcP2beta gene loci allowed the construction of an improved Trypanosoma cruzi expression vector. Gene 239, 217–225.
Vincent, I.M., Creek, D.J., Burgess, K., Woods, D.J., Burchmore, R.J., Barrett, M.P., 2012. Untargeted metabolomics reveals a lack of synergy between nifurtimox and eflornithine against Trypanosoma brucei. PLoS Negl. Trop. Dis. 6, e1618.
WHO/NTD, Crompton, D.W.T., Daumerie, D., Peters, P., Savioli, L., 2010. Working to Overcome the Global Impact of Neglected Tropical Diseases : First WHO Report on Neglected Tropical Diseases. World Health Organization, Geneva, Switzerland.
Wilkinson, S.R., Kelly, J.M., 2009. Trypanocidal drugs: mechanisms, resistance and new targets. Expert Rev. Mol. Med. 11, e31.
Yun, O., Priotto, G., Tong, J., Flevaud, L., Chappuis, F., 2010. NECT is next: implementing the new drug combination therapy for Trypanosoma brucei gambiense sleeping sickness. PLoS Negl. Trop. Dis. 4, e720.